EUROPEAN COMMISSION

HORIZON 2020 PROGRAMME - TOPIC H2020-LC-BAT-2019
Strongly improved, highly performant and safe all solid-state batteries for electric vehicles.

GRANT AGREEMENT No. 875189

SAFELiMOVE – Deliverable Report

<< D9.3 – Assessment of developed battery cell >>

Deliverable No.	SAFELiMOVE D9.3	
Related WP	WP9 << Multiscale-Multiphysics modelling >>	
Deliverable Title	Assessment of developed battery cell	
Deliverable Date	2023-12-31	
Deliverable Type	REPORT	
Dissemination level	Public (PU)	
Written By	Mark Junker (RWTH)	2023-12-08
Checked by	Arpit Mishra (ABEE)	2023-12-19
Reviewed by (if applicable)	Elixabete Ayerbe (CID)	2023-12-19
Approved by	María Martínez Ibañez (CICe)	2023-12-21
Status	final	2023-12-21

Disclaimer/ Acknowledgment

This project has received funding from the European Union's Horizon 2020 research and innovation programme under grant agreement No 875189. The information and views set out in this publication does not necessarily reflect the official opinion of the European Commission. Neither the European Union institutions and bodies nor any person acting on their behalf, may be held responsible for the use which may be made of the information contained therein.

Publishable summary

This document summarizes the results of modelling related research activities performed by ISEA at RWTH Aachen University as part of EU Horizon 2020 project SAFELiMOVE. In this project, the consortium developed and fabricated a ceramic polymer hybrid electrolyte all-solid-state-battery aiming to increase energy density and safety for automotive applications. With its modelling efforts, RWTH aimed to assess the viability of the cell produced for such an application and to identify shortcomings and potentials for further improvement and development.

As a variety of cell formats (coin, pouch monolayer, 1 Ah pouch and 3 Ah pouch) containing materials from different levels of development have been assembled within the project, this report covers the evaluation of cells at multiple stages of development. However, the focus lies on the evaluation of the gen1 (level 2 materials) and gen2 (level 3 materials) 1 Ah pouch cells as those cells have undergone the largest variety of aging tests and therefore provide most data for lifetime evaluation.

To allow for an extensive evaluation of the battery cell, three main aspects have been evaluated via simulations: Cell performance, thermal behavior, and ageing behavior. All those aspects have been evaluated using the open source ISEA Framework, a framework for simulations of equivalent circuit models combined with a thermal model and an ageing model developed by ISEA at RWTH Aachen university.

For each of those three sub-models, a modelling-based parametrization toolchain has been established making use of the limited amount of data available for the cell developed and allowing for facilitated updating to accommodate for the agile development of the cell continuously introducing and combining materials and designs for new cell iterations.

To generate an equivalent circuit model for the performance simulation, EIS measurements were simulated using a 3d-capable Doyle-Fuller-Newman type P2D model and subsequently, a 2RC equivalent circuit model was fitted to the simulation results. For the thermal parameters, a spreadsheet-based tool was developed calculating the effective heat capacity as well as the effective thermal conductivity both within and across the plane of the electrode sheets, based on available literature data on the individual compounds and materials. For the aging model, aging tests performed within the project on 1Ah pouch cells were evaluated and the main ageing mechanisms were calculated using empirical ageing models obtained from literature, and adapting the parameters included to fit the data from the ageing tests performed.

Both the simulations performed by RWTH, and the electrical battery tests performed by various partners within the project suggest that further improvement is necessary to fulfil the criteria for an application of the cell developed within the project in an electric vehicle. Regarding cell performance, simulations show that the ionic diffusivity of the conducting salt within the solid-state electrolyte might be the limiting factor for cell performance in terms of C-rate capability. C-rates above C/10 (depending on the material level) tend to lead to full polarization and depletion of conductive salt within the solid electrolyte at one of the electrodes, thereby limiting the current that can be provided by the cell over an extended amount of time.

Regarding the thermal behavior, the solid-state cell shows thermal parameters comparable to a liquid electrolyte cell, because the polymer electrolyte, which forms the bottleneck for heat transport across the electrode plains, behaves like a liquid electrolyte regarding thermal conductivity. As the realistic operating current of the cell is limited to low C-rates, significant heating of the cell is not an issue despite the increased internal resistance of the cell, as the resulting heat generated can be easily transported out of the cell. This is further underlined by the fact that the cell is meant to be operated at a temperature of 60 °C, meaning that the heat generated can be used to partially compensate for heat loss of the battery system to the environment. In case of an increase of the compatible C-rate of the cell, with no reduction of the internal resistance, heat management might become much more relevant.

Although the reproducibility of the ageing tests performed within the project is quite low, an ageing model has been set up based on the cyclic and calendar ageing tests. The resulting simulations show that besides

the rate capability, the cycle life of the cells might be the most significant factor prohibiting the use of the battery cell at the current level of development from being used in an EV application. With a cycle life of only 140 equivalent full cycles, the cells would only allow for a total distance travelled of 56.000 km assuming a vehicle with an available range of 400 km.

Executive summary

There are no deviations from the initial description of the deliverable from the grant agreement. All results have been gathered within the planned time frame until project month 48.

Contents

Figures

Tables

1 Introduction

Deliverable 9.3 concludes the activities within task 9.4 aiming to evaluate the feasibility of the cells produced by the consortium of the SAFELiMOVE project for the intended use in automotive application, identifying shortcomings and presenting directions for further improvements in the materials and cell design. As the number of available cells within the project was strongly reduced compared to initial plannings, parametrization of the models applied in this task was performed mostly from inputs from other work packages, like WP3 focusing on the materials, WP5 focusing on performance of smaller tests cells and WP7 performing ageing tests with the developed battery cells.

The evaluation of the battery cells was based on three critical aspects: cell performance, thermal behavior, and ageing behavior. These were thoroughly assessed using a parametrization toolchain leading into the ISEA Framework, an open-source platform developed by RWTH Aachen University. This framework integrates simulations of equivalent circuit models, thermal dynamics, and ageing patterns. Each aspect was scrutinized through dedicated sub-models, employing a parametrization toolchain designed to accommodate the evolving cell iterations.

Creating an equivalent circuit model involved simulating EIS measurements using a sophisticated Doyle-Fuller-Newman type P2D model. This was followed by fitting a 2RC equivalent circuit model to these simulation outcomes. Thermal parameters were derived through a tool that calculated effective heat capacity and thermal conductivity within and across electrode sheets based on existing literature. Ageing models were established by evaluating tests on 1 Ah pouch cells, utilizing empirical ageing models adjusted to fit the project's data.

Both simulations and electrical battery tests indicated that further enhancements are necessary for the cell's application in electric vehicles. Performance simulations highlighted potential limitations due to the ionic diffusivity of the conducting salt within the solid-state electrolyte, especially concerning C-rate capability. Additionally, ageing tests indicated a challenge regarding cycle life, potentially inhibiting the cell's current development level from being viable for EV applications. The projected cycle life of only 100 equivalent full cycles limits the total distance the cell could facilitate to approximately 50,000 km for a vehicle with a 500 km range.

In conclusion, this deliverable successfully demonstrated the potentials and shortcomings of the final design iteration of the cell and provides valuable insights for future research to design a solid-state cell in accordance with automotive demands. However, the low reproducibility of the tested cells and lower number of overall test conditions turn into a lower prediction accuracy than expected.

2 Modelling Toolchain for Cell Assessment

To assess the feasibility of the SAFELiMOVE cell for an automotive application, a modelling tool chain has been set up capable of reproducing performance, thermal and ageing simulations. The overall tool chain as well as the individual submodules will be further evaluated in the following subsections.

2.1 Toolchain Overview

This deliverable presents an electro-thermal lifetime model for the SSB developed within the SAFELiMOVE project. An overview of the different steps necessary to develop such a model is illustrated in Figure 1.

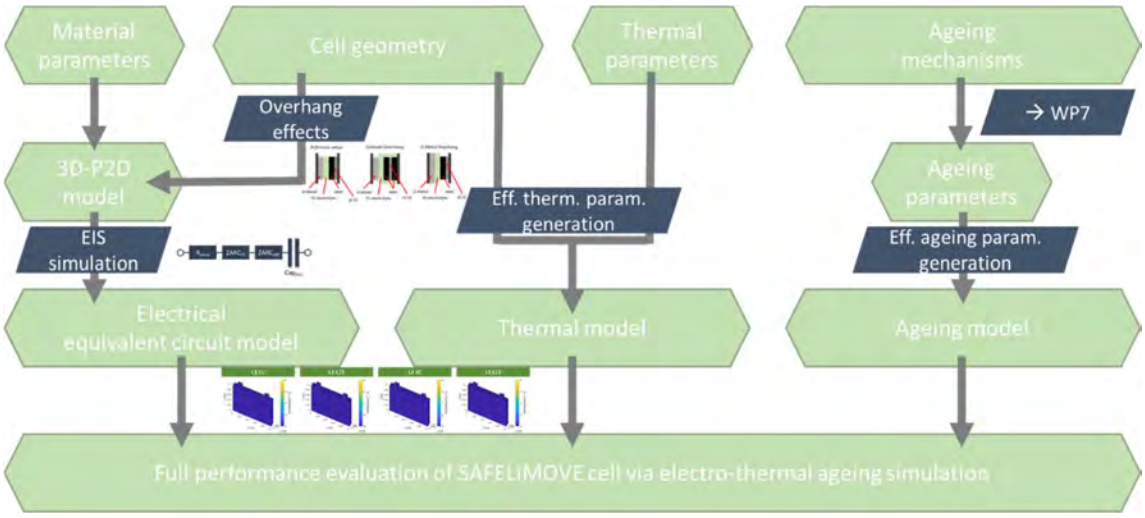

Figure 1: Interconnection of modules developed by RWTH for evaluation of SAFELiMOVE SSB

Aging model, thermal model and lifetime model are integrated within one singe modelling framework developed by ISEA at RWTH Aachen. This modelling framework is set open-source and available under the name *ISEA Framework*. Electrical performance simulations are based on equivalent circuit model simulations. The equivalent circuit model can be defined individually using different equivalent circuit elements such as resistors, RC elements and ZARC elements. For parametrization of the equivalent circuit model, a fitting of the equivalent circuit model parameters to impedance data is performed. Whilst using measured impedance data on cell level would result in the most accurate results, this procedure relies on the availability of an actual manufactured cell for testing and no direct link between the material properties and cell design and the cell performance during electrical simulation can be drawn. For this reason, an additional parametrization step including the physico-chemical P2D model from Task 9.1 has been introduced. This step includes the generation of artificial impedance data from electrochemical battery simulations which can be used afterwards for parametrization of the equivalent circuit model. Although this procedure is less accurate than directly using measured impedance data, it provides the flexibility to adjust physically meaningful cell parameters in the electrochemical model and thereby investigate the influence of those parameters on the equivalent circuit model parameters and on the subsequent electrical performance simulation. Besides the material properties, also the cell geometry has an influence on overall performance and especially overhang effects can have an influence on cell behaviour during the upscaling process. Therefore, also the influence of different overhang configurations on the impedance spectrum of the cell has been investigated via simulations.

The thermal model included within the ISEA framework is a finite volumes-based model directly interacting with the electrical model to resolve the spatial distribution of heat generation within the battery cell. It is based on effective thermal parameters, as no substructures within the battery cell such as electrodes or the electrolyte are considered in the model. This is due to limitations in complexity and computational power to achieve acceptable simulation times. Therefore, the effective heat capacity and the effective thermal conductivity in each direction must be either measured with a cell or calculated based on an

additional model. To allow the assessment of the influences of different design parameters on the thermal parameters, the modelling approach was chosen, aggregating cell geometry and material parameters of the individual cell compounds to effective thermal parameters.
For the ageing model, however, such a calculation of the cell level ageing parameters based on cell design and material parameters is not possible, as the relations between materials, geometry and ambient conditions are much more complex. Therefore, a direct calculation of the ageing parameters is not possible. Instead, ageing parameters are determined based on ageing tests performed within the project, and empirical equations are used to depict the ageing behaviour. In the simulation framework, electrothermal simulations are performed for a defined load profile and ageing factors are calculated. Subsequently, ageing is linearly extrapolated over a longer time horizon and the electrothermal simulations are repeated for that point in time. By this procedure, use phases of several years can be simulated making use of detailed load profiles whilst keeping computational costs low.

2.2 Performance Model

2.2.1 Physico-Chemical Battery Model

The foundation of the electrical performance model lies in a physico-chemical P2D model adapted for simulations of solid-state batteries within task 9.1. To cover the hybrid solid state electrolyte, effective transport parameters are implemented, which can be either measured on material samples or calculated using the models from task 9.2. Creating a framework to implement these models for overall evaluation of the SAFELiMOVE cells, a 3D-capable Newman type P2D model was implemented by RWTH, based on an electrical network providing excellent adaptability and capabilities of adding further features. The model is set up in C++, to allow for fast computing and to achieve real-time capability. RWTH also added features to the model to allow for simulation of lithium metal electrodes. Furthermore, an adaptive implicit solver was added to the P2D model to cover both short-term and long-term simulations with adequate accuracy and computation time. Simulations were validated using a set of data obtained from Literature for a 7.5 Ah pouch cells manufactured by Kokam. Figure 2 shows the comparison of measured and simulated voltage profile applying a current profile based on WLTP 1 test cycle. This model also is the basis for all further investigation of transport parameters in the hybrid electrolyte.

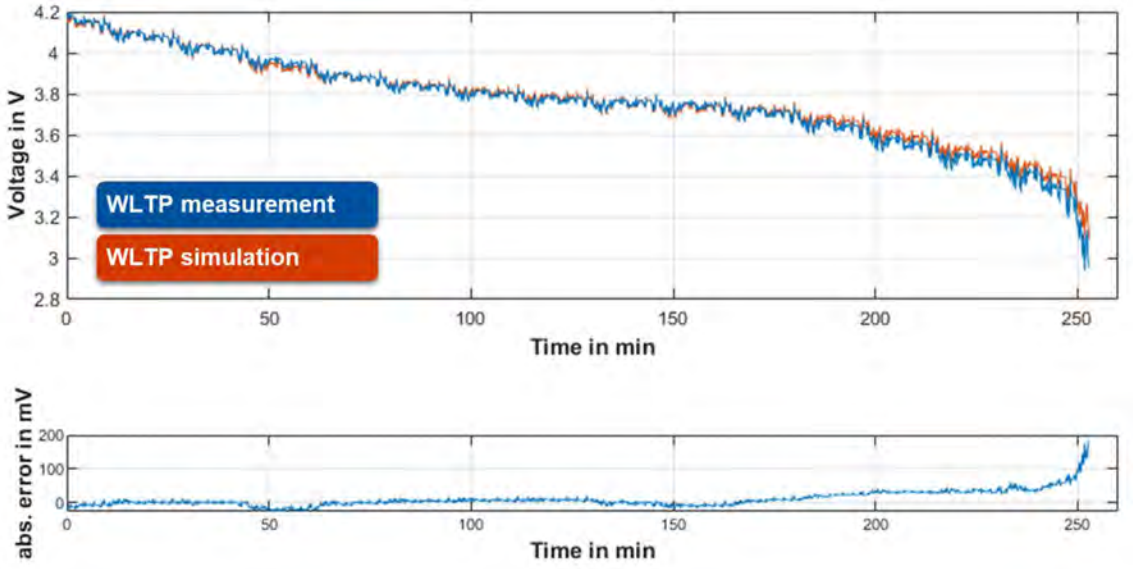

Figure 2: Comparison of measured and simulated data for a 7.5 Ah pouch cell using the P2D model developed by ISEA.

2.2.2 Overhang Model

The electrode overhang is a geometric cell parameter which can strongly affect the cell performance, and which is subject to adaptations during the upscaling process. RWTH investigated the influence of different types of overhang on the cell performance by simulations. For this purpose, the P2D model described in the previous section was adapted to allow simulations in cylindrical coordinates in three dimensions. The modeling approach developed was then validated comparing the lithiation of the backside overhang of graphite vs. Li metal coin cells in experiment and simulation. The experiments were performed using graphite, as this allows to optically investigate the SOC by color evaluation. Experiments and simulations were performed for a wide range of parameter sets (end voltages of 150 mV / 100 mV / 10 mV, holding times of 2 / 6 / 12 / 24 days, back side coated / double side coated, calandered / uncalandered, operation mode CV / 0-current / cycling). The results show good accordance between experiments and simulations, as shown in Figure 3, and the modeling approach therefore was validated. The lithiation process of the overhang can be separated into a diffusion limited and a potential driven phase. The initial diffusion limitation thereby results from a depletion of conductive salt in the overhang. A further sensitivity analysis of design parameters shows that active material porosity, overhang size and conductive salt diffusion coefficient in the electrolyte heavily affect the overhang behavior. Results have been published as part of the Battery Power Conference 2022.

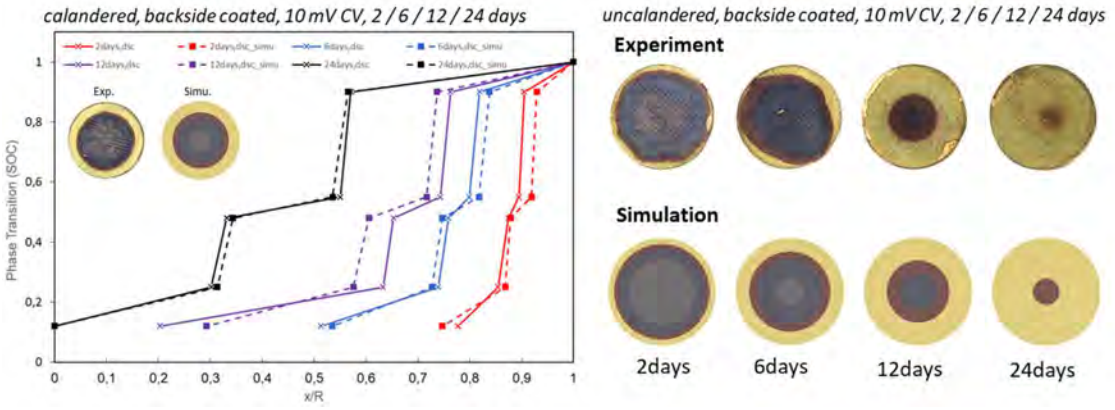

Figure 3: Model validation for the overhang simulation: Comparison of simulation and experimental results

The application of the derived overhang model on SAFELiMOVE materials shows significant influences of cathode overhangs whereas Li metal overhangs are negligible. The low Li salt diffusion coefficient, however, leads to very long time constants for the cathode overhang, thus restricting the relevance of a theoretical cathode overhang in an SSB for typical battery applications.

Figure 4 shows the simulated impedance spectra of coin cells with SAFELiMOVE materials. For the cathode overhang, a double-side coated cathode is investigated, with the same amount of active material in the overhang as in the active area of the cell. For the anode overhang, a lithium metal chip with larger diameter is simulated. The resulting impedance spectra show an additional semi-circle at very low frequencies for the cathode overhang and nearly no changes in the impedance spectrum for the anode overhang. The cathode overhang can be parametrized in the equivalent circuit model by a serial connection of a capacity and a resistor, in parallel connection to the voltage source resembling the OCV. In conclusion, a cathode overhang can have an influence on the amount of cyclable Li and cell capacity, but only over very long resting times, in the range of months to years. As for the final SAFELiMOVE cell design a setup with anode overhang is chosen, and as the fraction of anode overhang on the total active area of the cell becomes smaller in larger format cells, overhang effects can be neglected for all following investigations.

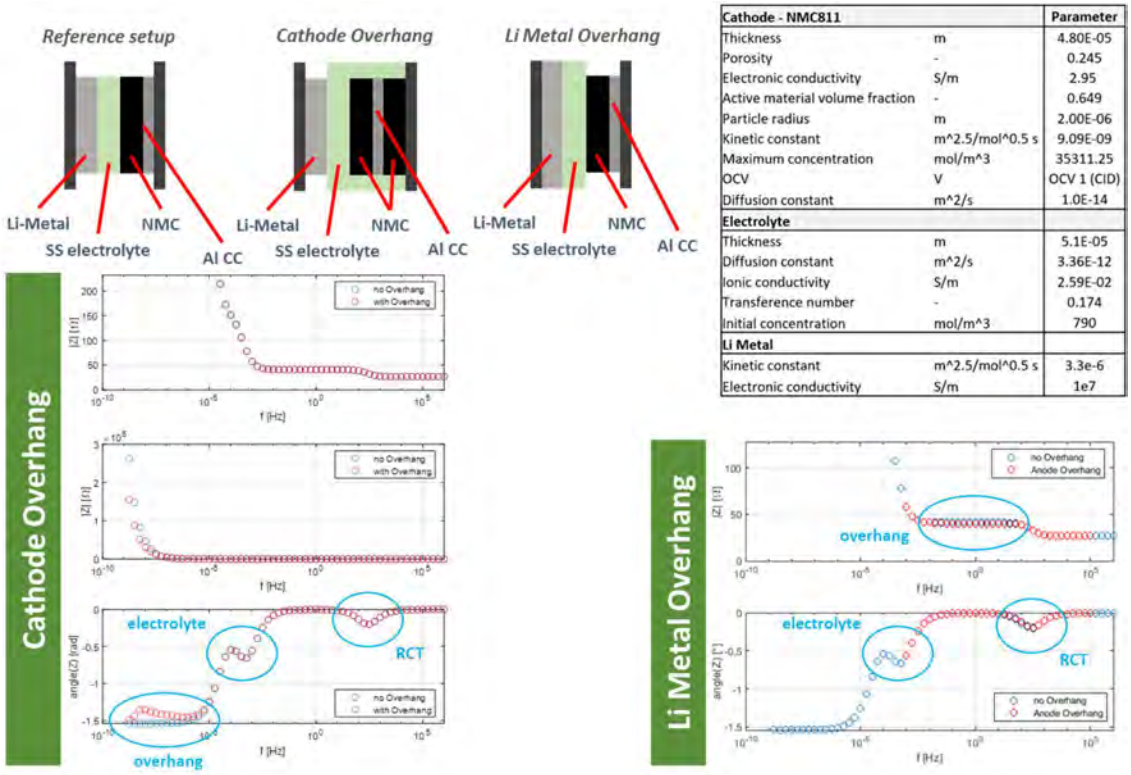

Cathode - NMC811		Parameter
Thickness	m	4.80E-05
Porosity	-	0.245
Electronic conductivity	S/m	2.95
Active material volume fraction	-	0.649
Particle radius	m	2.00E-06
Kinetic constant	m^2.5/mol^0.5 s	9.09E-09
Maximum concentration	mol/m^3	35311.25
OCV	V	OCV 1 (CID)
Diffusion constant	m^2/s	1.0E-14
Electrolyte		
Thickness	m	5.1E-05
Diffusion constant	m^2/s	3.36E-12
Ionic conductivity	S/m	2.59E-02
Transference number	-	0.174
Initial concentration	mol/m^3	790
Li Metal		
Kinetic constant	m^2.5/mol^0.5 s	3.3e-6
Electronic conductivity	S/m	1e7

Figure 4: Influence of anode and cathode overhang on the impedance spectrum of a coin cell

2.2.3 Performance Evaluation with the Physico-Chemical Model

To assess the feasibility of transferring physico-chemical simulations into the equivalent circuit model and to identify possible limitations, C-rate-tests were simulated based on the L1 and L2 material parameters and on an artificial set of parameters optimized for improved performance. In all parameter sets, conductive salt diffusion is the main limiting factor of cell performance. Therefore, conductive salt depletion is the reason for reduced extractable capacity at high C-rates. As this is a nonlinear effect that is not covered by equivalent circuit models, the latter will be only valid for C-rates lower than C/10 for L1 materials and lower than C/4 for L2 materials. However, this limitation is not critical as the C-rate-regime not covered by the equivalent circuit models is of no practical use, due to a short cell life when cycling at these C-rates. Results of the C-rate-test and the simulated conductive salt distribution after charge and discharge for L1 and L2 materials are presented in Figure 5.

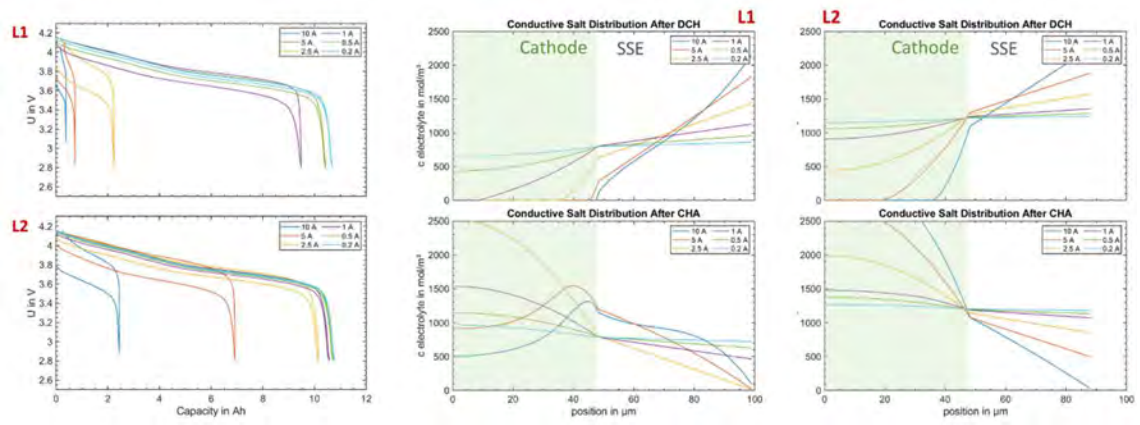

Figure 5: C-rate-simulation of L1 and L2 material (left); conductive salt distribution in the electrolyte after charge and discharge for L1 material (centre); conductive salt distribution in the electrolyte after charge and discharge for L2 material (right).

2.2.4 Determination of equivalent circuit parameters

To allow for a simultaneous evaluation of electrical and thermal battery behavior as well as battery ageing, the parameters describing the SAFELiMOVE battery cell must be transferred into an equivalent circuit-based modelling environment provided by RWTH. A tool for simulating the virtual EIS spectra, based on a P2D model, was developed by RWTH, to transform adaptations of easily interpretable physical and geometry-based cell parameters into an equivalent circuit model. This allowed investigating the effect of different battery parameter sets on the overall cell performance. Figure 6 shows the simulated Nyquist plot of a 10 Ah cell using L1 and L2 materials, as well as the optimized parameter set. A comparison with EIS data measured with three LG MJ1 18650 cells in parallel connection, also resulting in 10 Ah capacity, shows that the L2 material parameter set, and the optimized parameter set can reach impedance values close to those of liquid electrolyte battery cells.
As the simulated impedance spectrum shows two semicircles, an equivalent circuit model with two ZARC elements, an ohmic impedance, and a capacitor to depict the OCV behavior, was selected for model parametrization. An illustration of the equivalent circuit model and the resulting fitting parameters are depicted in Figure 7. As the shape of the OCV and the capacity of the cathode was not changed between the different material level simulations, the same value for the OCV related capacity would be expected for all simulations. As L1 materials show a higher value, a suboptimal fit can be expected.

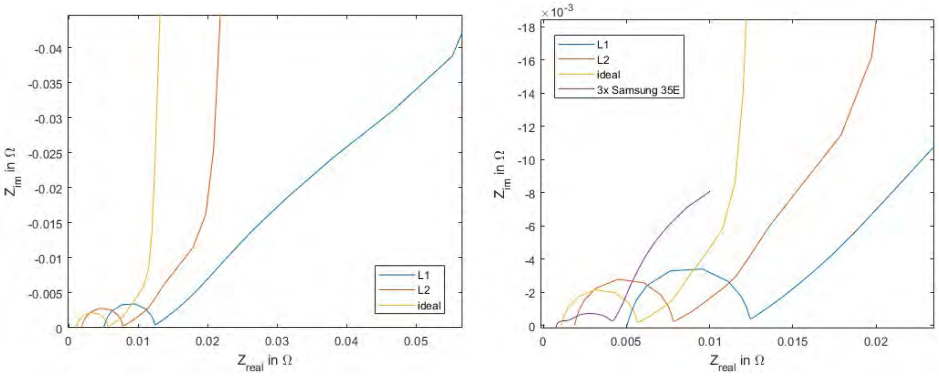

Figure 6: EIS spectra obtained from physico-chemical battery simulation for a 10 Ah cell with L1-, L2-, and optimized parameter set (left); comparison of these EIS spectra with the EIS spectrum measured with 3 LG MJ1 18650 cells in parallel connection (10 Ah)

	L1	L2	ideal
R_{serial} [mΩ]	5.1	1.9	1.1
R_{CT} [mΩ]	7.5	6.2	4.3
R_{Diff} [mΩ]	63.2	14.6	6.6
Cap_{OCV} [Ah/V]	19.2	16.6	16.2
	bad fit		

Figure 7: Fitting results for a 2 ZARC equivalent circuit model for 10 Ah cells based on L1, L2 and a theoretical set of optimized materials

2.2.5 Equivalent circuit model based electrical simulations

Simulations were performed using the ISEA Framework, to allow for a combined electrical, thermal, and ageing related simulation. Figure 8 depicts the simulation procedure for electrical simulations within the model: All parameters describing the equivalent circuit model are loaded into the framework via an .xml file (1) and the desired load profile (either current or power) is loaded as .csv file. For each time step, the load profile is evaluated (2) and all equivalent circuit parameters are calculated from the lookup tables provided, based on the system parameters SOC and temperature (3). Subsequently, the equations for the equivalent circuit model are set up (4) and transformed into a matrix (5) to be solved by a solver. The resulting voltages and currents (6) are the written into an output file and used to adapt the state of the system for the next evaluation of the lookup tables.

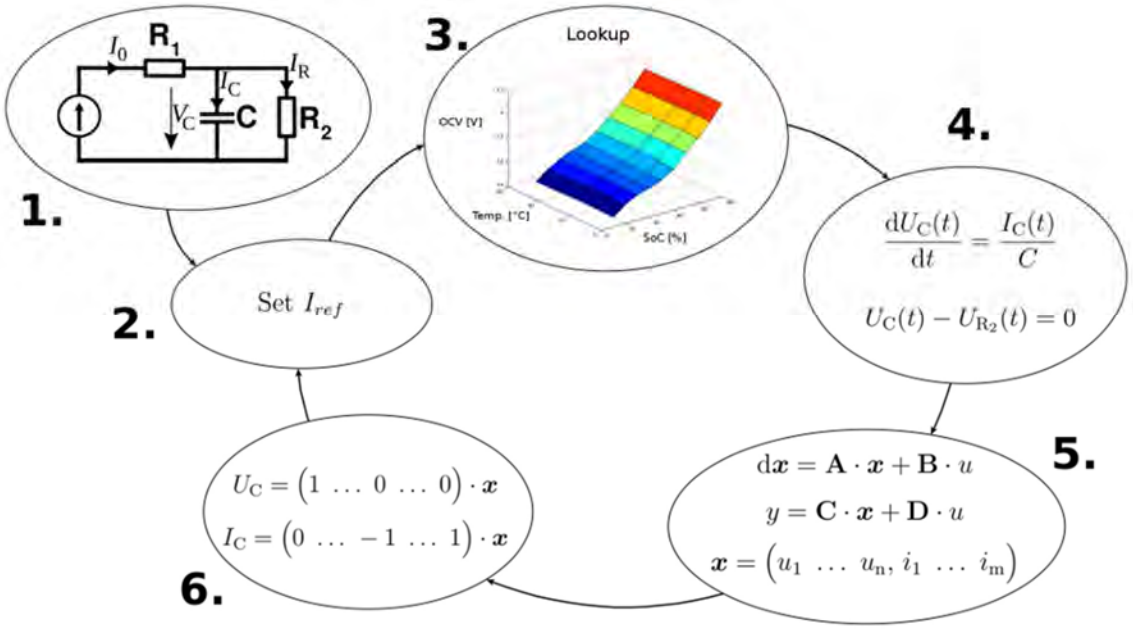

Figure 8: Simulation procedure of the ISEA Framework

2.3 Thermal Model

2.3.1 Identification of thermal parameters

To generate the electro-thermal ageing model depicted in Figure 1, the thermal capacity and the thermal transport parameters of the SAFELiMOVE cell need to be generated based on material properties available. Whilst the thermal capacity can be easily calculated based on the different material fractions within the cell, the heat transport through the cell is simulated based on effective transport parameters in cross-plane and in-plane direction of the electrode sheets. The approach of determination of those parameters is depicted in Figure 9.

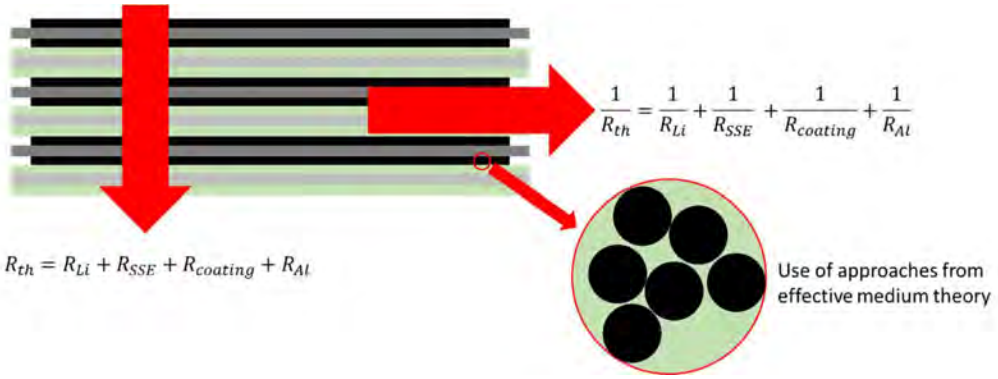

Figure 9: Calculation of effective thermal transport parameters

Literature values have been gathered for the heat capacity and thermal conductivity of all materials included in the SAFELiMOVE cell, to allow for a comprehensive overview of their thermal behavior. Table 1 presents the results of the thermal capacity and conductivity of a 10 Ah cell and of the cell components. The results are close to the values of a liquid electrolyte cell. This can be explained by the comparable thermal characteristics of liquid organic solvents and polymers. The strongest influence of the SSB investigated is related to the Li metal anode. The resulting thermal conductivity in the electrode plane is comparable to that of a graphite anode with a highly thermal conductive copper current collector, but exchanging the porous graphite with solid Li metal reduces the thermal resistance across the planes, thereby leading to increased thermal conductivity in the thickness dimension of the cell. The latter is the dimension with the lowest thermal conductivity. In total, 75% of the thermal resistance in through-plane direction is caused by the solid electrolyte and the remaining 25% by the porous cathode. The Li metal anode does not contribute significantly due to its high thermal conductivity.

Compound	Therm. Cap. [J/K]	Therm. Cond. [W/(m*K)]	Therm. Res. [(m²*K)/µW]
Cathode Coating	2.25	2.87	27.8
Cathode CC	0.36	230	0
Cathode Coating	2.25	2.87	27.8
SSE Ceramic	0.20	0.94	10.7
SSE Separator	0.35	0.31	81
Li Metal Anode	0.77	80	0.5
SSE Separator	0.35	0.31	81
SSE Ceramic	0.20	0.94	10.7
Total	**7.14**	**In plane: 25.1 Cross plane: 1.2**	**239**

Table 1: Contribution of each layer to the heat capacity and thermal conductivity of the SAFELiMOVE cell

2.3.2 Thermal simulations

Thermal modelling was performed in combination with the electrical simulations within the ISEA Framework. The thermal properties of the cell and the ambient conditions were therefore introduced into the .xml parameter file for the model. Simulation results for the thermal behavior for L1 and L2 material cells are depicted in Figure 10. Discharging currents of 1C and C/2 are chosen for the simulation, as these lead to an observable increase of temperature within the cell. Cooling is performed via convective cooling around the cell and via tab cooling, holding the tabs at a constant temperature of 25 °C. Owing to the low thickness of the cell, to large surface area for convective cooling and to the good thermal transport in direction of the tabs, no significant increase in temperature of the cell is noticeable at C/2 discharge with L2 materials. Consequently, no critical overheating of the cell during operation is expected, as the cells can operate only at lower C-rates. Furthermore, the cells will be operated at an elevated temperature of 60 °C, leading increased convective heat transport to the surrounding air. However, changes in cell design leading to capability for higher C-rates and a module design with low heat transport capability could have a severe impact on the thermal behavior of the cells during operation. This may lead to the need to reevaluate the thermal behavior of the cell.

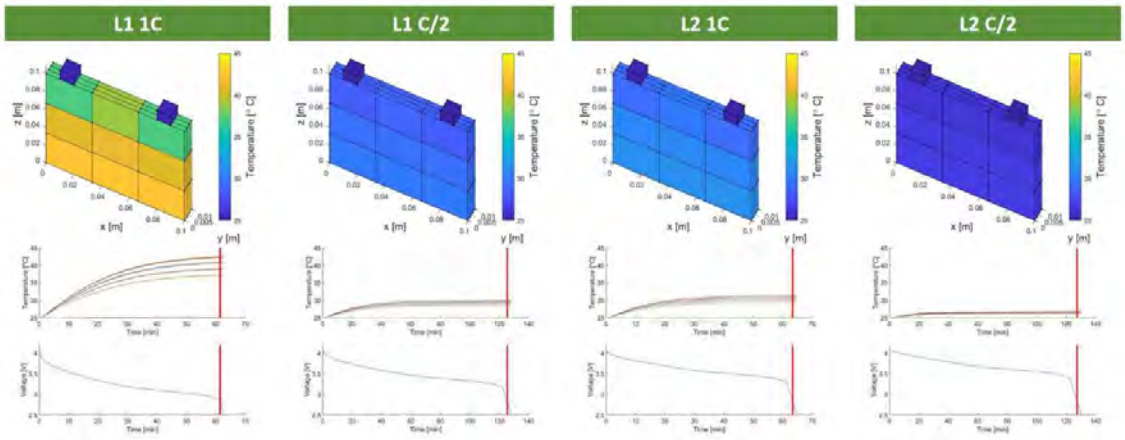

Figure 10: Results of electro-thermal modelling with L1 and L2 materials for 1C and C/2 discharge: Cooling by convective heat transport and tab cooling at 25 °C.

2.4 Ageing Model

The Ageing simulations within the electro-thermal ageing model rely mostly on the ageing results obtained within WP7. As the number of cells for ageing tests was limited and reproducibility of the test results could not be ensured for all tests, a simplified ageing model was set up to cover the very basic influences on ageing behavior.

2.4.1 Evaluation of ageing mechanisms

Battery ageing is observed either as an increase in the battery cell resistance or as a decrease in the available cell capacity. While an increase of the cell resistance (Ri) can be caused by processes related to the anode (Ri-A), the cathode (Ri-C) and the electrolyte (Ri-EL), the loss of cell capacity is normally caused by the loss of cyclable lithium (LLI), the loss of anode active material (LAM-A) or the loss of cathode active material (LAM-C). For the SSB developed within the SAFELiMOVE project, LLI and LAM-A are identical as the Li metal anode can fully contribute to the cyclable lithium. Since excess lithium is introduced into the SSB with the anode Li foil, LLI and LAM-A are not expected to be main contributing factors for loss of capacity of the investigated cell. The loss of cathode active material (LAM-C) leads to a steeper discharge curve with a lower total capacity, whereas the consumption of all active Li leads to a voltage curve resembling that of a pristine cell, with a sudden drop in voltage when all remaining lithium from the anode is intercalated. However, this behavior was not observed during electrical testing in WP7. Therefore, LAM-C and Ri are expected to be the main contributors to cell ageing for the SAFELiMOVE cells. Both effects can be caused by cyclic ageing or by calendar ageing without the influence of additional cycling. During calendar ageing, side reactions are the main cause of loss of capacity and increase of resistance. At the cathode, parts of the polymer electrolyte might oxidize, whilst at the anode the polymer is reduced, leading to the formation of surface layers, increasing the cell resistance, and possibly passivating parts of the cathode active material. Furthermore, reactions in the bulk electrolyte between the polymer and ceramic phase might cause increased surface resistance and decreased ionic conductivity. During cycling, protective passivation layers may degrade due to volume changes in the materials, leading to additional formation of degradation products, and further increasing the cell resistance. Furthermore, dead lithium might be formed during the plating reaction causing LLI. Finally, cathode particles can crack, leading to LAM-C, as cracked particles may lose their ionic connection in the process. An overview of the possible ageing mechanisms identified and their assumed dependencies on cell state of charge (SOC), depth of discharge (DoD), C-rate, and temperature, are presented in Table 2.

Calendar Ageing Kinetics		**Cyclic Ageing Kinetics**	
Capacity loss:		**Capacity Loss:**	
LLI:	**not of interest due to Li reservoir**	**LLI:**	**not of interest due to Li reservoir**
LAM-A:	**not of interest due to Li reservoir**	**LAM-A:**	**not of interest due to Li reservoir**
LAM-C:	**Passivation, might increase due to high Ni content and high operating temperature. → temperature and SOC dependent**	**LAM-C:**	**Particle cracking, loss of electric or ionic connection → temperature, SOC, C-rate and DoD dependent**
Resistance increase:		**Resistance increase:**	
Ri-A:	**SEI growth → temperature dependent, SOC independent**	**Ri-A:**	**SEI fracture ↓ , dead Li plating ↑ → temperature, C-rate and DoD dependent, SOC independent**
Ri-C:	**(?) CEI growth → temperature and SOC dependent**	**Ri-C:**	**Particle cracking ↓, loss of electric or ionic connection ↑ → temperature, DoD, C-rate and SOC dependent**
Ri-El:	**(?) Electrolyte decomposition → temperature dependent, SOC independent**	**Ri-El:**	**(?) Electrolyte cracking ↑ → temperature, C-rate and DoD dependent, SOC independent**

Table 2: Summary of identified possible ageing mechanisms to be introduced into the ageing model.

2.4.2 Evaluation of ageing models

To parametrize the ageing behavior of the SAFELiMOVE cells, an empirical ageing model was chosen. Such an empirical ageing model describes the loss rate of capacity and the increase rate of the internal resistance as function of ageing conditions. For cyclic ageing, one of the simplest approaches is a constant correlation between the capacity loss rate and the charge throughput, as described in Equation 1. $\frac{dC}{dQ}$ hereby describes the capacity loss in Ah per charge throughput in Ah (charge and discharge are considered positive charge throughputs) and *a* is the correlation factor. For integration of dependencies on DoD, SOC and C-rate, the simple model can be extended with additional terms taking into account changes in DoD (Equation 2), mean SOC (Equation 3) and C-rate (Equation 4). The simple approach presented here can be further modified using higher order equations with more parameters for fitting. However, a higher amount of fitting parameters also requires more testing conditions to determine those parameters. For temperature dependency, both linear and exponential approaches are common.

$$\frac{dC}{dQ} = -a$$

Equation 1

$$\frac{dC(DoD)}{dQ} = \frac{dC(DoD_0)}{dQ} \cdot (1 + b \cdot (DoD - DoD_0))$$

Equation 2

$$\frac{dC(SOC)}{dQ} = \frac{dC(SOC_0)}{dQ} \cdot (1 + c \cdot (SOC - SOC_0))$$

Equation 3

$$\frac{dC(CR)}{dQ} = \frac{dC(CR = 0)}{dQ} \cdot (1 + d \cdot CR)$$

Equation 4

$$\frac{dC(T)}{dQ} = \frac{dC(T_0)}{dQ} \cdot d \cdot T$$

Equation 5

$$\frac{dC(T)}{dQ} = \frac{dC(T_0)}{dQ} \cdot exp(b \cdot (T - T_0))$$

Equation 6

For the increase of the inner resistance, similar approaches can be applied with the difference that an increase in resistance is expected as shown in Equation 7.

$$\frac{dR_i}{dQ} = a$$

Equation 7

Calendar ageing can be described in similar ways by empirical equations with the main difference that the capacity loss and resistance increase is a function of time, instead of capacity throughput. A linear approach is presented in Equation 8 while Equation 9 displays an exponential approach with parameter *b* in a range from -1 to 0, and Equation 10 describes an approach limited by the SEI growth.

$$\frac{dC}{dt} = -a$$

Equation 8

$$\frac{dC}{dt} = -a \cdot t^b$$

Equation 9

$$\frac{dC}{dt} = -a \cdot \frac{1}{1 + b \cdot (C_0 - C)}$$

Equation 10

2.4.3 Parametrization of the ageing model

Parametrization of the ageing model is performed based on the cyclic and calendar ageing results on 1 Ah cells from WP7. As only a limited number of cells was available under different ageing conditions, not all parameters from the ageing models described in the previous section could be determined. Furthermore, results obtained with Gen1 and Gen2 cells will be combined, if necessary, to fill gaps in the data available.
Cyclic ageing tests performed by CID on Gen1 1Ah cells at C/10 and displayed in Figure 11 show strong influences of the upper cut-off voltage on the cycle life, with only 20 cycles until 80% SoH for a cut-off voltage of 4.35 V, and between 60 and 110 cycles until 80% SoH for a cut-off voltage of 4.2 V. This strong decrease in cycle life correlated with a comparably small increase of DoD, however, is most certainly attributed to strong damage to the cathode material at those voltages and ageing mechanisms which should not occur during normal operation. Therefore, the cycling window from 3 V to 4.2 V is selected as 100% DoD, and the cells with 4.35 V cut-off will not be used for model parametrization, therefore also not providing any correlation between DoD and ageing. With a mean charge throughput of 0.75 Ah per cycle and considering the best performing cell with 112 cycles until 80% SoH, an ageing factor of approximately **1 mAh/Ah** can be calculated for Equation 1. Cycling of a Gen2 cell by CID resulted in a similar cycle life as the Gen1 cell.

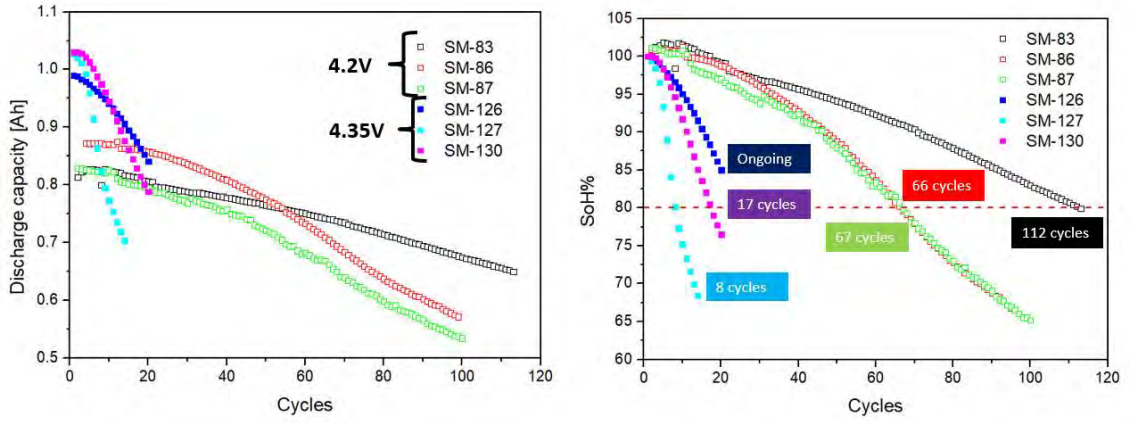

Figure 11: Cyclic ageing tests performed by CID on Gen1 1Ah cells at C/10

Additional cycling performed by TME with Gen1 cells at C/25, under similar conditions as those employed by CID, shows a decreased cycle life of 25 to 50 cycles until reaching 80% SoH, however at higher initial capacity. However, this effect is counterintuitive as lower C-rates are expected to lead to increased cycle life. For the Gen2 cells, TME determined an expected cycle life of 140 cycles, resulting in an ageing factor of approximately **0.8 mAh/Ah**. This decrease in ageing rate compared to the data obtained from CID could be related to a C-rate dependency of the ageing. Nonetheless, low comparability between the different

tests makes it impossible to draw a final conclusion. All ageing data can be found in Figure 12 and Figure 13.

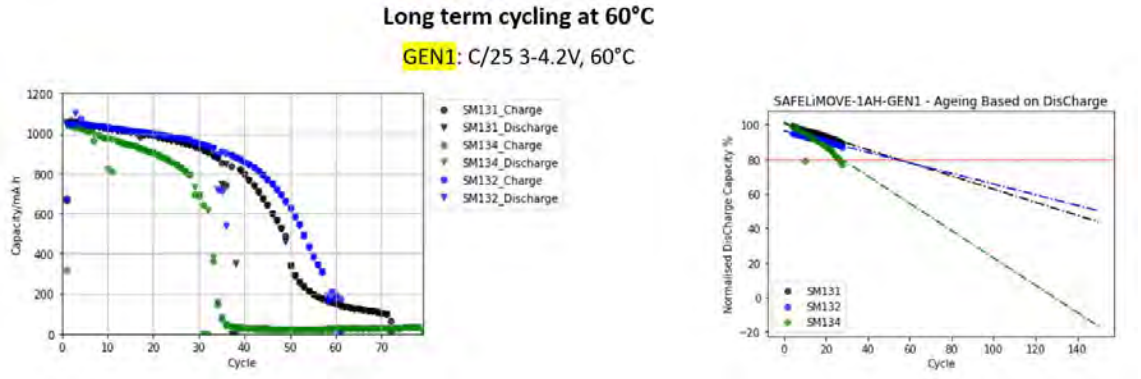

Figure 12: Cyclic ageing tests performed by TME on Gen1 1Ah cells at C/25

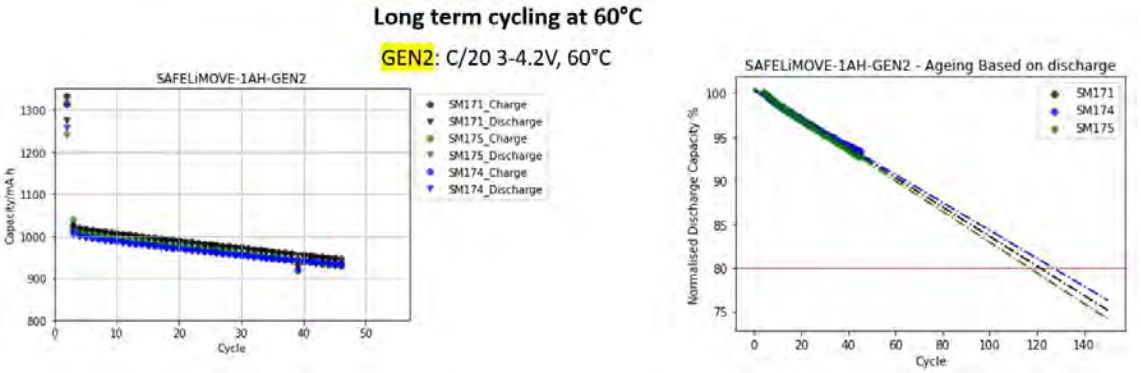

Figure 13: Cyclic ageing tests performed by TME on Gen2 1Ah cells at C/20

Calendar ageing tests were performed by ABEE with Gen1 1Ah cells and the results are displayed in Figure 14. In theory, different SOC and temperature conditions for ageing allow for a detailed calendar ageing model, but comparing the resulting ageing rates leads to inconsistencies. In general, high SOC values and high temperatures should lead to increased ageing. The results obtained, however, show the strongest ageing at 50% SOC. Evaluating the cell aged at 50% SOC and 60 °C, a calendar ageing rate of 3.6 mAh/day can be calculated. In comparison, cyclic ageing at TME at C/25 only caused a capacity loss of around 0.8 mAh/day whilst cycling. Calculating a calendar ageing rate from the tests performed at 80% SOC yields a more reasonable ageing rate of 0.7 mAh/day which, however, would still cover most ageing observed in the cyclic ageing tests performed at TME.

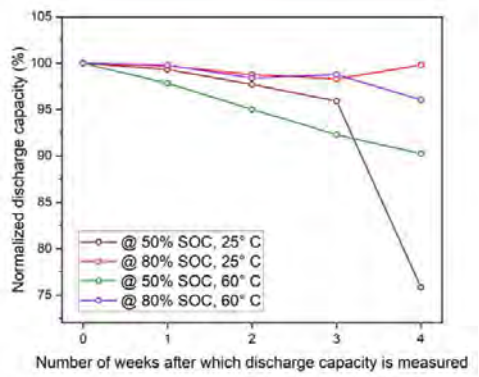

Figure 14: Calendaric ageing tests performed by ABEE on Gen2 1Ah cells

In conclusion, the parametrization of the ageing models suffers from low comparability and reproducibility off the cells tested and therefore does not allow for the generation of detailed ageing models. For cyclic ageing, an ageing rate of 0.8 mAh/Ah can be used resembling the best-performing cell and for calendar ageing an aging rate of 0.7 mAh/day might be a worst-case approximation although the actual value must be assumed smaller.

2.4.4 Ageing simulations

Bringing together the electrical performance model, the thermal model, and the ageing model, a full lifetime simulation for the SAFELiMOVE cell was performed for an automotive application. To best fit the limited rate capability of the cell, a purely urban drive profile according to WLTP 1 was selected and repeated twice for each trip, resulting in a total trip distance of 16.2 km and a driving duration for the trip of 34 min. For each day, a total of two trips are assumed: one starting at 7:30 and one starting at 17:00. With an assumed vehicle range of 400 km in an urban environment, the 32.4 km of daily use results in a use of 8.1% of the available energy of the battery cell and the WLTP cycle is rescaled to the capacity of the 1 Ah cell accordingly. Assuming a 50 kWh vehicle battery and making use only of slow, single phase charging at home, with a charging power of 3.5 kW, a charging event with a duration of 1 h and 10 min is added to the drive cycle, starting at 17:40. The resulting synthetic load profile is displayed in Figure 15. For reduction of computational costs, the drive profile is assumed the same for each day of the year and battery ageing is reevaluated every 90 days. This scenario results in a total distance traveled per year of approximately 11800 km.

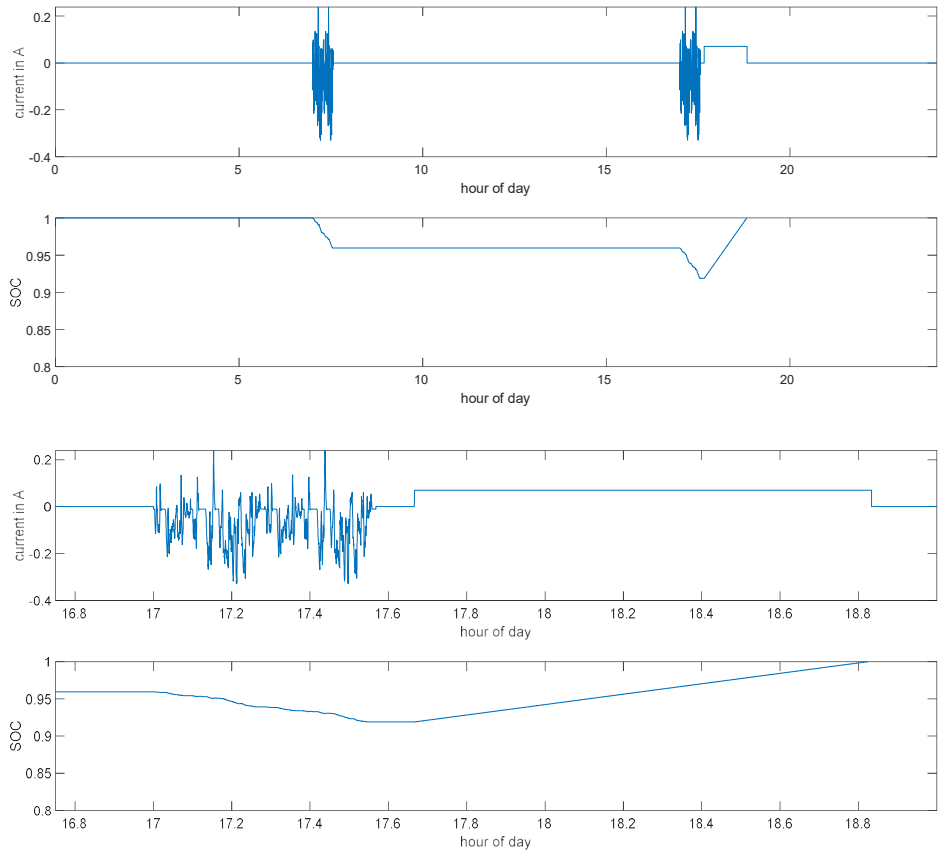

Figure 15: Synthetic daily use profile

As only very limited ageing parameters could be extracted from the ageing results of the cells, 3 scenarios are investigated combining different parameters for calendar ageing rate and DoD dependency. SC1 is the base scenario with the results from the parametrization, SC2 adds the calendar ageing as predicted by ABEE, and SC3 decreases the ageing caused by very small DoD to a quarter of the original cyclic ageing rate.

Scenario	SC1	SC2	SC3
Cyclic ageing rate	0.8 mAh/Ah	0.8 mAh/Ah	0.8 mAh/Ah
Cyclic ageing DoD dependency	0 %/%$_{DoD}$	0 %/%$_{DoD}$	0.75 %/%$_{DoD}$
Calendaric ageing rate	0 mAh/day	0.7 mAh/day	0 mAh/day

Table 3: Scenario overview

The resulting ageing trajectories for the three scenarios are depicted in Figure 16. Although the cell only has a limited cycle life of 140 full cycles, the large battery capacity in combination with the short daily drive profile leads to a predicted lifetime of nearly four years to 80% SOH or nearly 8 years to 60% SOH. Assuming reduced ageing at small cycles, this lifetime might even be extended beyond 10 years. In contrast, when considering calendar ageing as determined by ABEE, a lifetime of less than one year could be reached.
In conclusion, a lifetime sufficient for an automotive application might be in reach for the SAFELiMOVE cell, however only by restricting power demands to urban drive profiles, assuming slow charging and only expecting a yearly distance travelled of less than 12000 km.

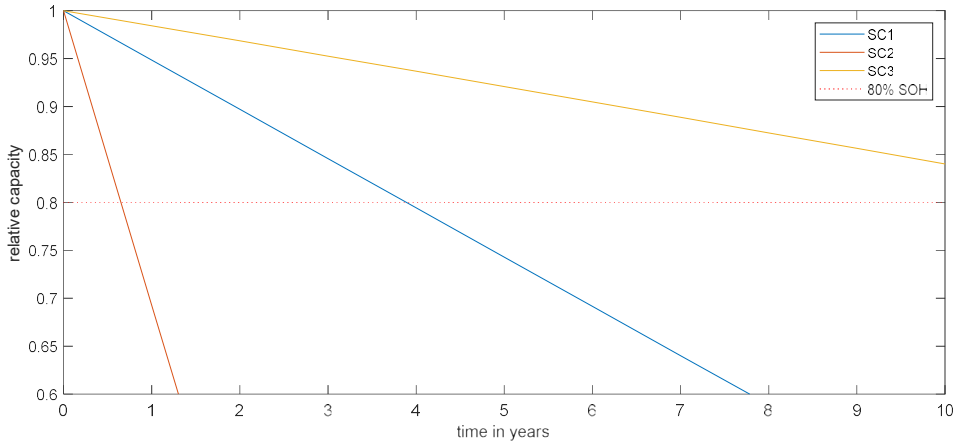

Figure 16: Simulated ageing trajectories for the different scenarios

3 Conclusions and Recommendations

In conclusion, this deliverable successfully created a modelling toolchain to assess the viability of the SAFELiMOVE cell in its current design iteration for automotive applications. The two major factors restricting the use in an EV are the rate capability and the cyclic lifetime.

For rate capability, simulations have demonstrated that the low lithium salt diffusivity in the solid-state electrolyte leads to polarization of the electrolyte, partial use of the active material and strongly inhomogeneous current distribution. Those effects limit the extractable capacity of the cell and furthermore can cause fast degradation during cycling at elevated C-rate. As those effects already become significant at C-rates between C/5 and C/10, further improvement of the salt diffusivity in the solid-state electrolyte or of the transference number of the Li Ions is necessary to obtain a cell that can fulfill the demands of fast-charging and provision of high power during discharge.

For cell ageing, cyclic ageing seems to be the bottleneck for EV application, although calendar ageing results are not conclusive and calendar ageing could potentially also restrict the lifetime of the battery in an EV. As loss of cyclable lithium and loss of the Li metal anode are directly connected, the main possible degradation mechanisms for a solid-state cell are Loss of Lithium Inventory (LLI) Loss of Cathode Active Material (LAM-C) and rise of the inner resistance (Ri). Concluding from cycling and postmortem results, the cell capacity is limited by the amount of available cathode active material, therefore LAM- therefore is the main limiting ageing mechanism. As Li is available in excess and there is no differentiation between loss of lithium and loss of anode active material, an electrode specific investigation of the ageing is not required, and cell ageing can be depicted by a decrease of available capacity and an increase in internal resistance. For use in an EV application, assuming a range of 400 km, a cycle life of at least 500 full cycle equivalents would be required for a total range of 200.000 km.

Although still showing obstacles to overcome for integration in an EV, key issues have been addressed within this deliverable and especially for EVs with lower demands on fast charging and power provision, the SAFELiMOVE cell could become a valid alternative with improvements in reach of technical feasibility.

Appendix A- Acknowledgement

The author(s) would like to thank the partners in the project for their valuable comments on previous drafts and for performing the review.

Project partners:

#	Partner	Partner Full Name
1	CICe	CENTRO DE INVESTIGACION COOPERATIVA DE ENERGIAS ALTERNATIVAS FUNDACION, CIC ENERGIGUNE FUNDAZIOA
2	SCHOTT	SCHOTT AG
3	UMICORE	UMICORE
4	HYDRO-QUEBEC	HYDRO-QUEBEC
5	SAFT	SAFT
6	RENAULT SAS	RENAULT SAS
7	TME	TOYOTA MOTOR EUROPE NV
8	IKERLAN	IKERLAN S. COOP
9	CEA	COMMISSARIAT A L ENERGIE ATOMIQUE ET AUX ENERGIES ALTERNATIVES
10	CIDETEC	FUNDACION CIDETEC
11	TUB	TECHNISCHE UNIVERSITAT BERLIN
12	RWTH AACHEN	RHEINISCH-WESTFAELISCHE TECHNISCHE HOCHSCHULE AACHEN
13	ABEE	AVESTA BATTERY & ENERGY ENGINEERING
14	LCE Srl	LIFE CYCLE ENGINEERING SRL
15	UNIRESEARCH BV	UNIRESEARCH BV